LOW VOLTAGE ACTUATION OF HIGH FORCE ELECTROSTATIC LATCHES

Joseph T. Greenspun and Kristofer S.J. Pister
University of California, Berkeley
Berkeley Sensor and Actuator Center

ABSTRACT

Using a 6 V MEMS relay and multi-lever mechanism we have demonstrated the release of 2 µJ of mechanical energy from a MEMS spring. Additionally, the same MEMS spring was held and released using an alumina-coated lever array. The addition of this alumina deposition allows for the creation of higher force electrostatic latches than would be possible in a standard single-mask SOI process. With as little as 38 V applied, these latches can restrain springs applying forces up to 173 mN.

KEYWORDS

Low voltage, electrostatic latch, high force actuator

INTRODUCTION

Micromachined actuators are often sought out for their ability to operate at low power. However, this low power operation is often in direct opposition to the actuator's ability to produce large forces at high speeds. Thus, actuators with these requirements often utilize an energy storage and rapid release mechanism. This allows the low power actuators to slowly store energy over time and release it all at once.

Rapid large force mechanical events at the MEMS scale are used in applications ranging from jumping microrobots [1] to self-destructing ICs [2]. In both cases, the large forces are restrained for some period of time until the stored mechanical energy is eventually released. Rodgers created a MEMS "crossbow" capable of storing and releasing 19 nJ of energy [3]. The stored energy was released by sinking an unreported amount of current through a polysilicon filament. Churaman [1] created a mechanism capable of storing and releasing 100 µJ of energy with a manual release mechanism. A lower force latching mechanism was developed for the Texas Instruments Digital Micromirror Device [4]. These electrostatic latches ensure that the mirror is held in place between address cycles.

Electrostatics offer a promising solution for latching mechanisms due to their ability to operate at low voltages and near zero input power requirements. In this work, a single-mask silicon-on-insulator (SOI) process is built upon to allow for the creation of sub-lithographic gaps filled with a high-κ dielectric, greatly reducing the operating voltage of these electrostatic latches.

FABRICATION AND DESIGN

Limits of Single-Mask SOI

An energy storage and rapid release mechanism was designed and fabricated to study microfracture using a single-mask SOI process [5]. This mechanism, shown in the top of Figure 1, works by rotating the lever arm toward the high voltage contact using a probe tip. This operation loads the horizontal beams and stores a predetermined amount of energy in the system once the lever arm makes contact with the gap stops. These gap stops protrude slightly from the high voltage contact and thereby define, through lithography, the final gap between the lever arm and this contact. A large voltage is applied across the lever arm and the contact which keeps the springs loaded in their high-energy state until this voltage is released.

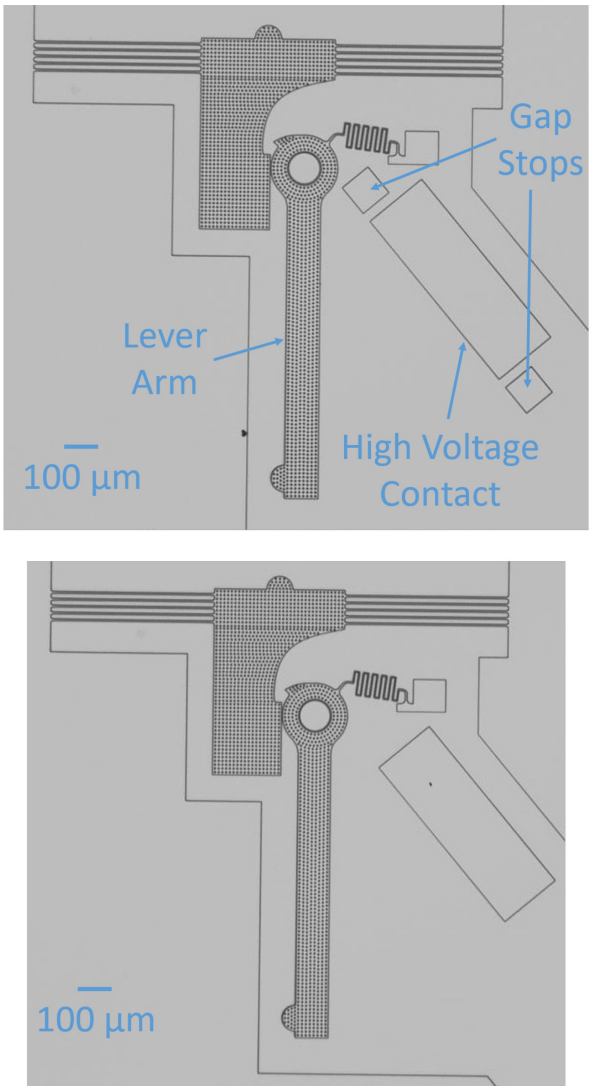

Figure 1: Two versions of the electrostatic latching mechanism. (top) A gap stop based design requiring no additional processing steps. (bottom) A high-κ dielectric based design that does not use gap stops.

For the system to be in static equilibrium, the moment produced by the electrostatic force of the latch

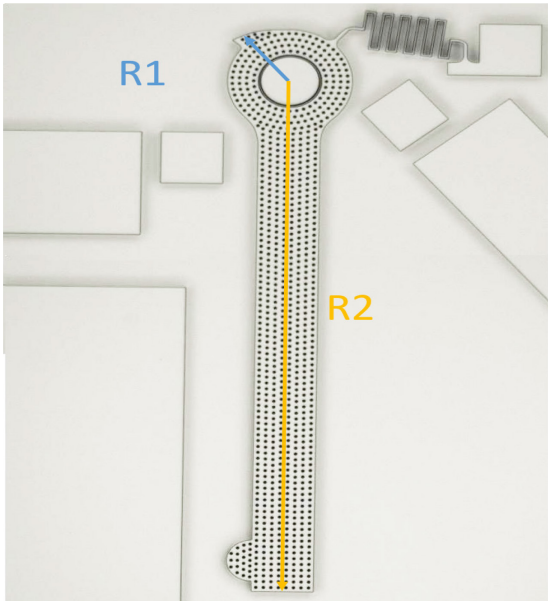

Figure 2: The lever arm that provides mechanical advantage to amplify the weak electrostatic force. Here, R1 is 100 µm and R2 is 1000 µm.

must balance the moment due to the restoring force of the springs. The electrostatic force is given by the following equation:

$$F_{es} = \frac{1}{2}\epsilon_0 \epsilon_r A \frac{V^2}{d^2}$$

Here the distance between the electrodes, *d*, is limited by the deep reactive ion etcher (DRIE) used to etch the device layer silicon. From previous work [5], it was determined that a gap (defined by the offset of the gap stop and the high voltage contact) of less than 0.5 µm could not be reliably etched into the device layer. This single-mask process does not allow for the deposition of a dielectric so the gap will be air-filled during operation, thus the relative permittivity is 1. These characteristics of the process severely limit the electrostatic forces attainable for this structure.

The electrostatic force on its own would not be sufficient to directly balance the restoring force of the springs, so one or more lever arms is used to amplify this weak force. The mechanical advantage gained with a single lever arm, shown in Figure 2, is roughly equal to half of R2, the centroid of the distributed electrostatic force, divided by R1. When multiple stages are used, the mechanical advantage increases to R2/R1 for every stage that is not electrostatically driven. In Figure 4, the mechanical advantage from the first three stages is R2/R1, and is roughly R2/(2*R1) for the fourth stage, leading to an overall mechanical advantage of ~$R2^4/(2*R1^4)$.

Process Modifications

The main limitations of the standard single-mask SOI process are the lack of a high-κ dielectric deposition and the relatively large minimum gap sizes, both of which limit the maximum electrostatic force. By slightly modifying the device design and adding a few processing steps, both of these limitations were removed and the electrostatic force increased dramatically.

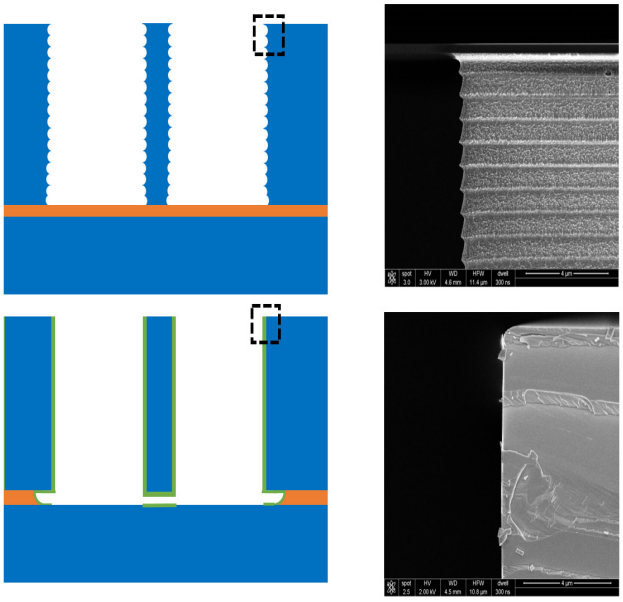

Figure 3: Salient features of process flow with corresponding SEM of fabricated structure. (top) Scalloped sidewalls of DRIE. (bottom) Final cross section with smoothed, alumina-coated sidewalls.

By removing the gap stops from the layout as in Figure 1 bottom, a conformal deposition of a dielectric can be performed to increase the relative permittivity of the gap material. This has an additional benefit in that the gap distance is now defined by twice the thickness of the deposited dielectric, as opposed to the mask offset between the gap stop and the high voltage contact. This gap distance should be minimized to allow for the highest electrostatic force at the lowest voltage, however an issue arises as a result of the DRIE process. This process produces scalloped sidewalls as shown in the cross-sectional image in the top right of Figure 3. These scallops have a pitch of roughly 750 nm and limit the minimum separation between the two sidewalls. The points of the scallops also act as field enhancement sites and can lead to electrical breakdown across the gap at a lower voltage than expected. To solve these problems an additional processing step is used to smooth out these features.

Lee showed that the scalloped sidewalls from the DRIE process could be transformed using a high temperature low pressure hydrogen anneal [6]. Lee found that when silicon was heated to 1100 °C in a hydrogen environment, the silicon atoms on exposed surfaces could surface diffuse and settle in a geometry that limited the surface energy, a smooth surface. The pressure, temperature, and duration of this hydrogen anneal were tuned to smooth any features with a radius of curvature less than 1 µm, while not significantly altering any feature larger than 1 µm.

The final process, while technically still a single mask process, adds the abovementioned processing steps to increase the electrostatic force of these latches. Starting with an SOI wafer with a 40 µm device layer, a 2 µm buried oxide, and a 550 µm handle wafer, the design is patterned and etched into the device layer silicon using DRIE. The high temperature hydrogen anneal is then performed at 1150 °C at 20 Torr for 10 minutes. The structures are

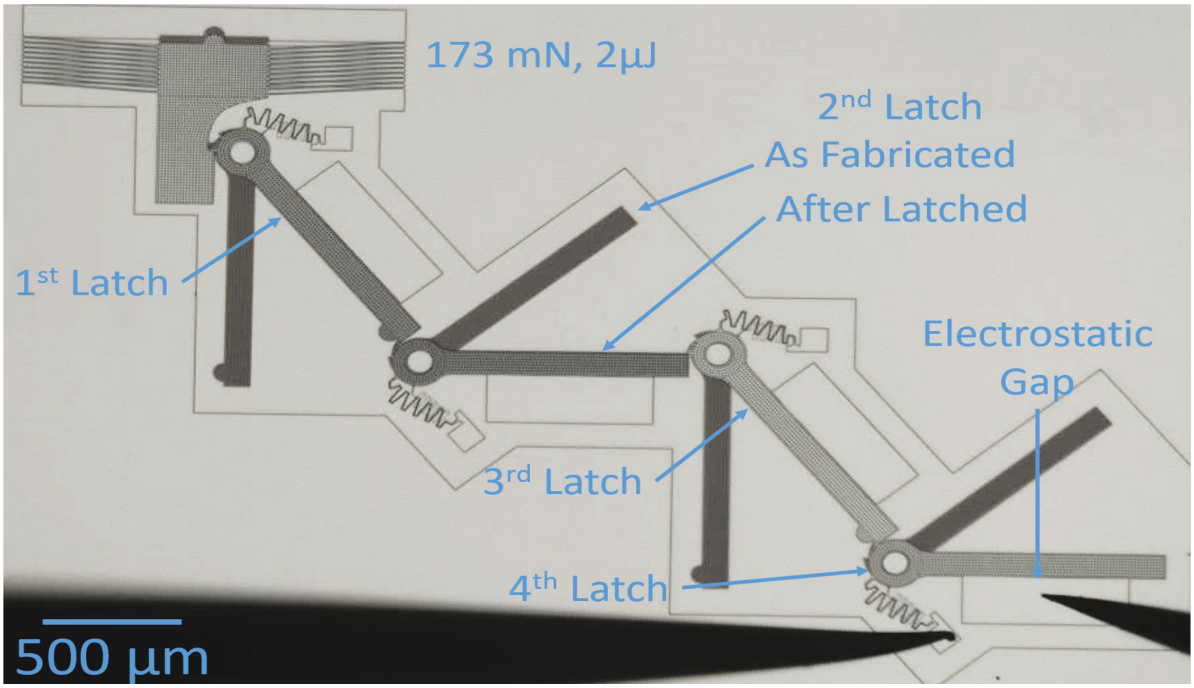

Figure 4: A four-stage alumina latch with 45 V applied across the electrostatic gap. The springs provide 173 mN of restoring force and store 2.0 µJ of mechanical energy. The shadowing is caused by a thin film of alumina still present under each lever arm's initial position.

released with a 5 µm oxide etch using vapor HF. The wafer is then placed in an atomic layer deposition (ALD) tool and 55 nm of alumina are deposited at 300 °C. Finally, an unmasked reactive ion etch (RIE) is performed to remove all alumina from the top surfaces in order to make electrical contact to the structures. Figure 3 shows a cartoon and SEM of a cross section after the DRIE step (top) as well as after the entire process is complete (bottom). It is important to note that since the ALD is performed after the structures have been released, all released structures will have alumina underneath them as shown in the bottom left cartoon.

RESULTS AND DISCUSSION

Devices were fabricated with a number of force amplification stages ranging from 1 to 8. Measurements were taken on each device to determine the minimum voltage required to restrain the springs. The force-deflection profile of these springs has been determined in previous work [5]. For single stage structures, shown in Figure 1, the lever arm is pushed toward the high voltage contact and a large potential is applied across the lever arm and the contact. The probe that originally engaged the lever arm is removed, and the latch is held in place by the applied potential alone. This voltage is reduced until the latch swings open; the last value at which the latch remained closed is considered the minimum latching voltage. For devices with two or more stages, such as the four-stage latch in Figure 4, each lever must be moved into place sequentially before the final lever is engaged and the voltage applied. The alumina shadowing left behind by the process can be seen clearly in Figure 4.

The results of these experiments can be seen in the plot in Figure 5. Each latch was tasked with restraining the same energy storage mechanism, which exerted a force of 173 mN and stored 2.0 µJ of energy. The theory curves are generated using the electrostatic force equation with the proper mechanical advantage factor. This electrostatic moment must balance the moment caused by the energy storage mechanism as well as the serpentine spring that attaches each lever arm to its anchor. This serpentine spring serves as the electrical connection to the lever arm, and provides the out-of-plane stiffness required to keep the lever from disengaging with its circular anchor. This spring deflects roughly 130 µm and has a stiffness of 64 N/m, which leads to a force of over 8 mN. The moment arm on this serpentine spring is comparable to that of the energy storage mechanism.

The main takeaway from the data shown in Figure 5 is that the additional processing steps help reduce the operating voltages of these switches immensely. The alumina gap latches require less than 30% the voltage required by the air gap latches. The data shows that the device-to-device variation of the latches that use air gaps is far greater than the variation in the alumina gap devices. The minimum gap size used in the air gap designs was set at 0.5 µm because this was the smallest gap that still gave reliable latch operation. At gaps smaller than this, devices tended to break down before they latched. The larger this gap, the more consistent the results, but the higher the minimum latching voltage is. The alumina gap devices on the other hand are especially precise, having a standard deviation of only a few volts in most cases. The combination of the non-irregular sidewalls and the finely controlled electrostatic gap helped lead to this more repeatable device.

Another difference between the two data sets is their deviation from the expected value predicted from theory. The air gap latches although varying wildly, match fairly well with the theoretical values. The alumina gap latches on the other hand all require about three times the

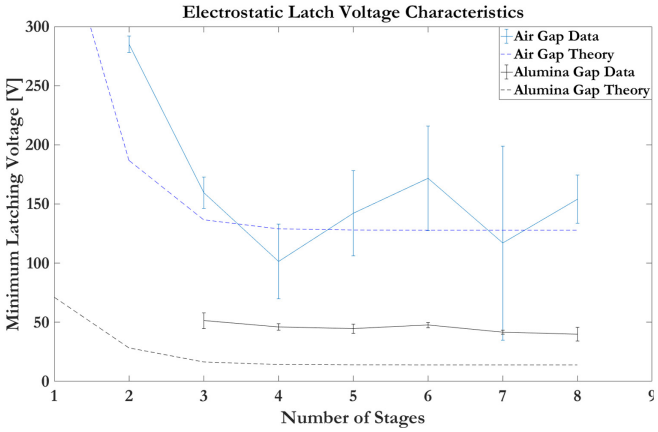

Figure 5: Plot of release voltage for both types of electrostatic latches.

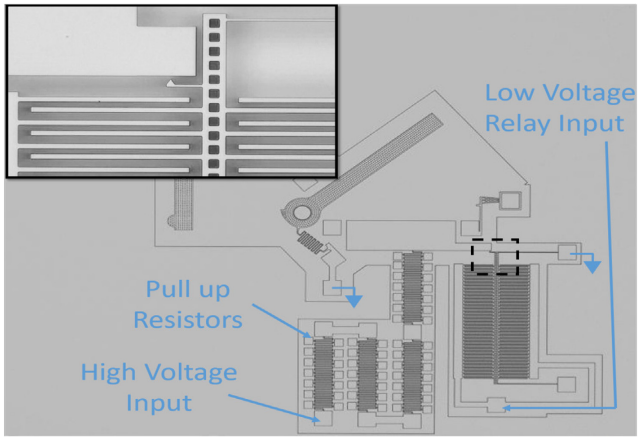

Figure 6: A low voltage relay capable of releasing an electrostatic latch with a signal of 6V.

expected theoretical voltage. One explanation for this difference is the misalignment between the lever arms and the high voltage contacts on the non electrically active stages. In layout, these are designed to line up exactly with each other however there is possibly some misalignment introduced by one of the additional processing steps. This misalignment could lead to an additional stiffness not accounted for, thus requiring more voltage than predicted by the model.

The theoretical curves as well as the alumina gap data in Figure 5 show there is a negligible reduction in latching voltage when adding more than 4 stages. These curves approach an asymptote equal to the voltage required to keep a single unloaded latch closed. This value is non-zero due to the stiffness associated with the lever arm's serpentine spring.

A device was designed and fabricated to create a low voltage latch in the standard single-mask SOI process. Figure 6 shows a two-stage latch that requires 175 V to remain latched. This 175 V signal is applied to the high voltage input and the latch will remain shut until the low voltage relay input is pulled high with a 6 V signal. This causes the grounded portion of the gap closing actuator, shown in the figure inset, to make contact with the high voltage contact, pulling it lower than the 175 V required to keep it closed due to the large pull-up resistor. While this still requires a large voltage to keep the latch closed, it can be triggered with a more reasonable 6 V input signal.

CONCLUSION AND FUTURE WORK

In this paper, we demonstrated two devices capable of triggering the rapid release of mechanical energy. A low voltage MEMS relay based design required a 6 V input signal and a constant high voltage rail of 175 V. An alumina-coated multi-lever system was able to restrain a 173 mN force with a single input voltage of 38 V. A high temperature hydrogen anneal and alumina deposition enabled a 3x decrease in the operating voltage of these electrostatic latches.

The latching voltage of these mechanisms can be further reduced by optimizing various components of the process. The serpentine spring can be made less stiff by increasing the number of meanders or their length. The thickness of the alumina coating can be reduced, increasing the capacitance of the electrostatic gap. Additionally, there are other ALD compatible materials that provide higher dielectric constants, such as TiO_2, that could potentially drive down operating voltages further. All of these process changes are being explored for the next iteration of devices.

ACKNOWLEDGEMENTS

We would like to thank the UC Berkeley Marvell Nanolab Staff for their help during this project, as well as the DARPA VaPR program for providing funding.

REFERENCES

[1] Churaman, Wayne A., Aaron P. Gerratt, and Sarah Bergbreiter. "First leaps toward jumping microrobots." *Intelligent Robots and Systems (IROS), 2011 IEEE/RSJ International Conference on*. IEEE, 2011.

[2] Greenspun, J, Kahn, O., Kumar, R., Massey, T., Volkman, S., Wheeler, B., Pister, K.S.J., Subramanian, V., "Morphing Autonomous Gigascale Integrated Circuits: An Integrated Approach to Vanishing Programmable Resources" *GoMacTech* (2017).

[3] Rodgers, M. Steven, et al. "Microelectromechanical high-density energy storage/rapid release system." Symposium on Micromachining and Microfabrication. International Society for Optics and Photonics, 1999.

[4] Van Kessel, Peter F., et al. "A MEMS-based projection display." Proceedings of the IEEE 86.8 (1998): 1687-1704.

[5] Greenspun, J., Massey, T., Pister, K.S.J., "The MEMS Hammer, A tool to study microfracture" Hilton Head 2016 Solid State Sensor and Actuator Workshop Technical Digest (Hilton Head Island, SC)

[6] Lee, MCM, Wu, Ming C. (2006). "Thermal annealing in hydrogen for 3-D profile transformation on silicon-on-insulator and sidewall roughness reduction." Journal of Microelectromechanical Systems, 15(2), 338-343. UC

CONTACT

Joey Greenspun, greenspun@eecs.berkeley.edu